

## **Xenobiotic tracers uncover the gastrointestinal passage, cellular uptake and Ago2 loading of milk microRNAs in neonates**

**Short title:** Milk miRNA GI passage and cellular uptake

Patrick Philipp Weil<sup>1</sup>, Susanna Reincke<sup>1</sup>, Christian Alexander Hirsch<sup>1</sup>, Federica Giachero<sup>1</sup>, Malik Aydin<sup>1,2</sup>, Jonas Scholz<sup>3</sup>, Franziska Jönsson<sup>3</sup>, Claudia Hagedorn<sup>3</sup>, Duc Ninh Nguyen<sup>4</sup>, Thomas Thymann<sup>4</sup>, Anton Pembaur<sup>1</sup>, Valerie Orth<sup>5</sup>, Victoria Wünsche<sup>1</sup>, Ping-Ping Jiang<sup>4,6</sup>, Stefan Wirth<sup>2</sup>, Andreas C. W. Jenke<sup>7</sup>, Per Torp Sangild<sup>4</sup>, Florian Kreppel<sup>3</sup>, Jan Postberg<sup>1,\*</sup>

\*corresponding author

### **Authors and e-mail addresses:**

Patrick Philipp Weil	<a href="mailto:patrick.weil@uni-wh.de">patrick.weil@uni-wh.de</a>
Susanna Reincke	<a href="mailto:susanna.reincke@uni-wh.de">susanna.reincke@uni-wh.de</a>
Christian Alexander Hirsch	<a href="mailto:christian.hirsch@uni-wh.de">christian.hirsch@uni-wh.de</a>
Federica Giachero	<a href="mailto:federica.giachero@uni-wh.de">federica.giachero@uni-wh.de</a>
Malik Aydin	<a href="mailto:malik.aydin@uni-wh.de">malik.aydin@uni-wh.de</a>
Jonas Scholz	<a href="mailto:jonas.scholz@uni-wh.de">jonas.scholz@uni-wh.de</a>
Franziska Jönsson	<a href="mailto:franziska.joensson@uni-wh.de">franziska.joensson@uni-wh.de</a>
Claudia Hagedorn	<a href="mailto:claudia.hagedorn@uni-wh.de">claudia.hagedorn@uni-wh.de</a>
Duc Ninh Nguyen	<a href="mailto:dnn@sund.ku.dk">dnn@sund.ku.dk</a>
Thomas Thymann	<a href="mailto:thomas.thymann@sund.ku.dk">thomas.thymann@sund.ku.dk</a>
Ping-Ping Jiang	<a href="mailto:jiangpp3@mail.sysu.edu.cn">jiangpp3@mail.sysu.edu.cn</a>
Anton Pembaur	<a href="mailto:anton.pembaur@uni-wh.de">anton.pembaur@uni-wh.de</a>
Valerie Orth	<a href="mailto:valerie.orth@helios-gesundheit.de">valerie.orth@helios-gesundheit.de</a>
Victoria Wünsche	<a href="mailto:victoria.wuensche@uni-wh.de">victoria.wuensche@uni-wh.de</a>
Stefan Wirth	<a href="mailto:stefan.wirth@helios-gesundheit.de">stefan.wirth@helios-gesundheit.de</a>
Andreas C. W. Jenke	<a href="mailto:andreas.jenke@klinikum-kassel.de">andreas.jenke@klinikum-kassel.de</a>
Per Torp Sangild	<a href="mailto:pts@sund.ku.dk">pts@sund.ku.dk</a>
Florian Kreppel	<a href="mailto:florian.kreppel@uni-wh.de">florian.kreppel@uni-wh.de</a>
Jan Postberg	<a href="mailto:jan.postberg@uni-wh.de">jan.postberg@uni-wh.de</a>

<sup>1</sup>Clinical Molecular Genetics and Epigenetics, Faculty of Health, Centre for Biomedical Education & Research (ZBAF), Witten/Herdecke University, Alfred-Herrhausen-Str. 50, 58448 Witten, Germany

<sup>2</sup>HELIOS University Hospital Wuppertal, Children's Hospital, Centre for Clinical & Translational Research (CCTR), Witten/Herdecke University, Heusnerstr. 40, 42283 Wuppertal, Germany

<sup>3</sup>Chair of Biochemistry and Molecular Medicine, Faculty of Health, Centre for Biomedical Education and Research (ZBAF), Witten/Herdecke University, Stockumer Str. 10, 58453 Witten, Germany

<sup>4</sup>Comparative Pediatrics and Nutrition, Department of Veterinary and Animal Sciences, University of Copenhagen, Copenhagen, Denmark

<sup>5</sup>HELIOS University Hospital Wuppertal, Department of Surgery II, Centre for Clinical & Translational Research (CCTR), Witten/Herdecke University, Heusnerstr. 40, 42283 Wuppertal, Germany

<sup>6</sup>School of Public Health, Sun Yat-sen University, Guangzhou, China

<sup>7</sup>Klinikum Kassel, Zentrum für Kinder- und Jugendmedizin, Neonatologie und allgemeine Pädiatrie, Mönchebergstr. 41-43, 34125 Kassel, Germany

### **Grant support**

This study was funded by the HELIOS Research Centre (JP) and the NEOMUNE research program (PTS) from the Danish Research Councils. University of Copenhagen has filed a patent concerning the use of bovine colostrum for groups of paediatric patients. The authors have no other relevant affiliations or financial involvement with any organisation or entity with a financial interest in or financial conflict with the subject matter or materials discussed in the manuscript apart from those disclosed. No writing assistance was utilised in the production of this manuscript.

### **Abbreviations**

Adenovirus-type 5 (Ad5); gastrointestinal passage (GI passage); human intestinal epithelial cells (HIEC); necrotizing enterocolitis (NEC); post-transcriptional gene silencing (PTGS); RNA interference (RNAi); transcriptional gene silencing (TGS)

## **Correspondence**

Jan Postberg

Clinical Molecular Genetics and Epigenetics, Faculty of Health, Centre for Biomedical Education & Research (ZBAF), Witten/Herdecke University, Alfred-Herrhausen-Str. 50, 58448 Witten, Germany

e-mail: [jan.postberg@uni-wh.de](mailto:jan.postberg@uni-wh.de)

phone: +492028962544

fax: +492028962546

## **Disclosures**

All authors declare that there is no conflict of interests.

## **Preprint**

medRxiv.org: doi: <https://doi.org/10.1101/2021.08.24.21262525>

## **Transcript profiling**

The datasets generated and/or analysed during the current study are available in the NCBI BioProject repository as fastq.gz files of miRNA-seq and mRNA-seq (SubmissionIDs: SUB7584111/

SUB9897357/BioProject ID: PRJNA740153/URL: <https://www.ncbi.nlm.nih.gov/bioproject/740153>).

## **Word count**

2998 (comprising introduction, results and discussion, conclusions)

## **Synopsis**

We provide a line of evidence that vertical transmission of milk miRNA signals via GI transit towards responsive cells and systemic bloodstream distribution is possible. This will prompt the understanding about milk miRNA bioactivity with respect to neonatal intestinal maturation.

## **Abstract**

**Background and aims:** Exclusive breastfeeding is the best source of nutrition for most infants, but it is not always possible. Enteral nutrition influences intestinal gene regulation and the susceptibility for inflammatory bowel disorders, such as necrotizing enterocolitis (NEC). In modern neonatology it is observed that lactase activity increases during intestinal maturation, but formula-fed infants exhibit lower activity levels than milk-fed infants. Since human breast milk has a high miRNA content in comparison to other body fluids, it is controversially discussed whether they could influence gene regulation in term and preterm neonates and thus might vertically transmit developmental relevant signals.

**Methods:** Following their cross-species profiling via miRNA deep-sequencing we utilized dietary xenobiotic taxon-specific milk miRNA as tracers in human and porcine neonates, followed by functional studies in primary human fetal intestinal epithelial cells (HIEC-6) using Ad5-mediated miRNA-gene transfer.

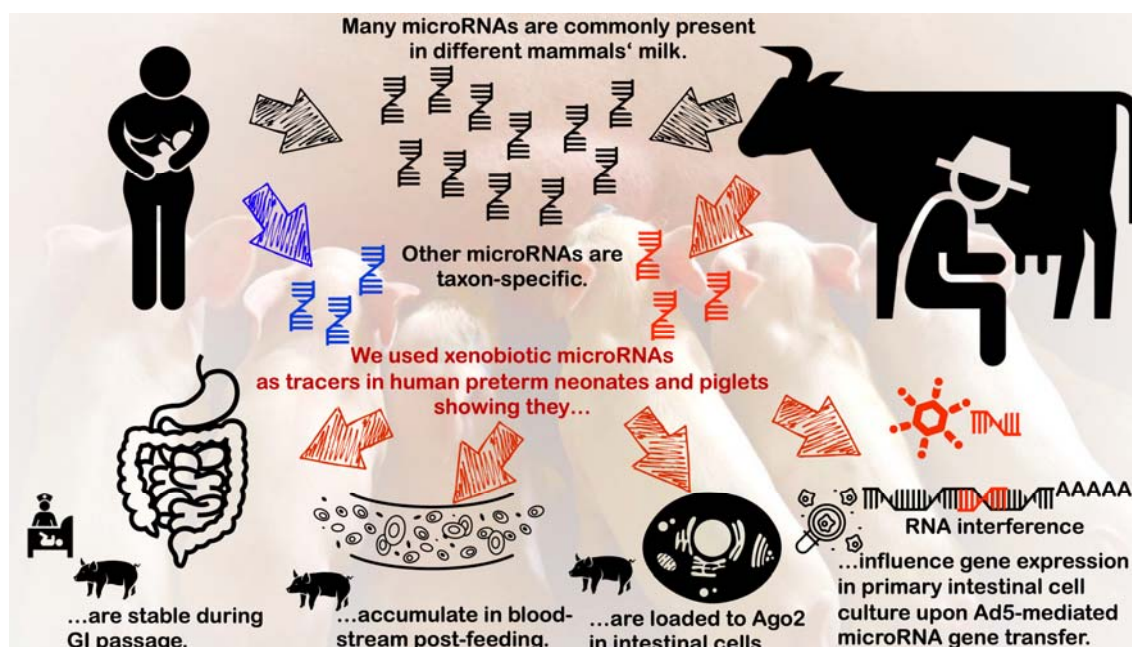
**Results:** Mammals have in common a large number of milk miRNAs yet exhibit taxon-specific miRNA fingerprints. We traced intact bovine-specific miRNAs from formula-nutrition in human preterm stool and 9 days after the onset of enteral feeding in intestinal cells of preterm piglets. Few hours after introducing enteral feeding in preterm piglets with supplemented reporter miRNAs (cel-miR-39-5p/-3p), we observed enrichment of the xenobiotic cel-miR in blood serum and in Ago2-immunocomplexes from intestinal biopsies. This points to a transmissibility of milk miRNA signals. We performed Adenovirus type 5-based miRNA-gene transfer into HIEC-6 and examined predicted bovine milk miRNA targets on the protein and transcriptome levels.

**Conclusions:** Results suggest that milk miRNAs could influence gene expression in intestinal epithelia of neonates under special conditions in vitro.

## **Key words**

intestinal maturation; enteral feeding; necrotizing enterocolitis; preterm delivery

## Graphical abstract



© Creative Commons Icons were downloaded from the Noun Project (<https://thenounproject.com/> [ 'breastfeeding' by Gan Khoon Lay from the Noun Project; 'milking' by Laymik from the Noun Project; 'digestive system' by Design Science, US, in the Organs Collection; 'bloodstream' by Oleksandr Panasovskiy, UA; 'cell' by Léa Lortal from the Noun Project; 'RNA' by Georgiana Ionescu from the Noun Project; 'pig' by parkjisun from the Noun Project; 'nursery' by Luis Prado from the Noun Project; 'arrow up' by Alex Muravev from the Noun Project; 'cancer cells' by dDara from the Noun Project; 'adenovirus' by Fariha Begum from the Noun Project]) and arranged for this graphical abstract.

## Introduction

Exploiting xenobiotic milk has a long history in human nutrition since the Neolithic revolution and left marks in contemporary human genomes. Whereas most native European hunter gatherers apparently exhibited lactase (LCT) non-persistence post-weaning, dairy farming practiced by immigrating Neolithic cultures came along with genetic adaptations associated with LCT persistence post-infancy. Apparently, domestication of mammals led to a beneficial niche construction, where those adaptations allowed to exploit xenobiotic milk as additional food source (1-5). Particularly bovine milk has a global role for human nutrition to date and in addition to fresh milk, industrialized dairy products play an important role in the global market (6), e.g. in the form of powdered milk or formula nutrition for neonates. In preterm neonates it is observed that LCT activity increases after the begin of enteral

feeding with formula-fed infants exhibiting lower lactase activity levels than milk-fed infants (7). One possible explanation is that milk vs. formula feeding can differently influence the epigenetic LCT regulation. In a preterm piglet model supplementation with formula or bovine colostrum led to differential intestinal gene expression patterns, when compared to total parenteral nutrition (8). Importantly, enteral feeding influences the risk for necrotising enterocolitis (NEC) in preterm infants. NEC susceptibility increases in premature infants and piglets receiving xenobiotic formula milk when compared to breast milk/colostrum feeding (9-12). However, the molecular background of nutrition-dependent differences in gene regulation remains concealed.

Whereas the chromatin structure controls transcriptional gene silencing (TGS), post-transcriptional gene silencing (PTGS) utilizes RNA interference (RNAi), sometimes at important nexus in hierarchical gene regulatory networks (Figure S1). RNAi key factors are non-coding microRNAs (miRNAs) interacting with Argonaute (Ago) protein family members to target specific mRNAs via base-pairing of their 5'-seed (13-15). Perfect or near-perfect base-pairing promotes the decay of targeted mRNAs, whereby translational repression seems to be another mechanism of PTGS (16). In cells, miRNAs fulfil important regulatory functions, but they occur also ubiquitously in body fluids. Among different body fluids, human breast milk seems to exhibit the highest total miRNA concentration (17). Also, miRNAs are found in processed milk- products, such as formula milk (18). There is an ongoing debate in science and society about possible adverse effects of milk consumption with particular emphasis on bovine milk and in some instances focussing the controversy on its miRNAs content (19-21). But the discussion suffers from a lack of comparative and experimental data about the biological relevance of milk miRNAs. One exception was an elegant approach looking at the intestinal uptake of milk miRNAs in mmu-mir-375-knockout and mmu-mir-200c/141-knockout mice offspring, which received milk from wild-type foster mothers. Here, no evidence for intestinal epithelial uptake of miRNA and/or its enrichment in blood, liver and spleen was seen (22). Contradicting results were obtained from another study that simulated infant gut digestion *in vitro* and analysed the uptake of human milk miRNAs by human intestinal epithelial crypt-like cells (HIEC) deriving from foetal intestines at mid-gestation. Here, milk miRNA profiles remained stable after digestion and evidence for the uptake of milk-derived exosomes in HIEC was reported (23). There is

an urgent need for further rigorous experimental data to inspire the debate and address the open problems: Are milk miRNAs functional, or are they a nucleo(t/s)ide source, only? We currently neither know whether milk miRNAs build a path of vertical signal transmission from mother to the newborn nor whether interferences of xenobiotic miRNAs with human target mRNAs can influence developmental pathways (24). We thus aimed to interrogate the potential relevance of human and xenobiotic milk miRNAs in specific situations in early human life.

## **Results and discussion**

We followed the working hypothesis that breast milk miRNAs could fulfil a regulatory signalling function, which could be most important within a discrete perinatal ‘window of opportunity’ during the introduction of enteral feeding, when the infant’s intestine develops as an environment-organism interface to coordinate microbiome homeostasis. Moreover, we considered that intestinal immaturity in preterm neonates could provide a clinically significant niche for (xenobiotic) milk miRNA influence.

### *Mammals have in common a large number of milk miRNAs yet exhibit species-specific milk miRNA fingerprints*

We determined milk miRNA profiles of human (hsa), cattle (bta), goat (cae), and sheep (ogm) to clarify a potential role of miRNA molecules in dietary milk. Furthermore, milk miRNAs from pig (ssc), okapi (ojo), horse (eca), donkey (eas), cat (fca), and dog (clu) were considered to possibly derive an evolutionary context of their profiles, for example putative milk miRNA differences between omnivores, herbivores, and carnivores (Figure 1A). The top 100 milk miRNAs from 21 specimens representing <90% of the total mapped miRNA read counts (92.40-96.39%) were visualized as heat map and dot plot (Figure 1B,C). Across all taxa we detected 1291 hairpin-like pre-miRNAs (pre-mir), whereby each single pre-mir could potentially give rise to two mature single-stranded mature miRNAs (miR) through processing of its guide (5p) and/or passenger (3p) strand. 139 of these pre-mirs occurred in all taxa.

Robustly, the heat map suggested a stable quantitative distribution of most miRNAs in most species' milk, whereby principal component analyses revealed somewhat separated clusters: Cluster 'blue' contained all human specimens, cluster 'green' contained all herbivores as well as dog, whereas pig and cat appeared somewhat separated (Figure S2). Using ANOVA for deeper investigation of the putative differences between hsa-miRs and bovid miRs, we identified only few differences with solely miR-192-5p being  $p < 0.0001$  and 3 miRs being below  $p < 0.05$  (miR-1246, miR-146b-5p, miR-4516). Similarly, few differences were seen, when we compared hsa-miRs vs. ssc-miRs, bovid miRs vs. ssc-miRs, omnivores miRs vs. herbivores miRs, omnivores miRs vs. carnivores miRs and herbivores miRs vs. carnivores miRs (Table S1).

Apart, numerous miRNAs were apparently shared by some taxa or occurred taxon-specific. Through their annotations and Blast searches in miRBase (25), we undertook an approach to systematically identify taxon-specific pre-mir and to analyse their non-overlapping or partially overlapping occurrence in different taxa (Table S2). For each taxon, we identified several hundreds of milk pre-mirs (carnivores:  $n=240$ ; bovinds:  $n=521$ ; human:  $n=679$ ; pigs:  $n=272$ ; equids:  $n=381$ ) (Figure 1D). Notably, 225 pre-mir were shared between humans and cattle. We found 440 pre-mir being human-specific, 270 being bovinds-specific and many more taxon-specific pre-mir (pigs [ $n=91$ ], equids [ $n=172$ ] and carnivores [ $n=240$ ]). We concluded that xenobiotic miRNAs could be exploited as tracers to study the gastrointestinal (GI) passage as well as systemic and cellular uptake in human or animal models.

#### *Cattle-specific milk miRNA can potentially target human mRNA*

To study the GI passage of milk miRNAs we selected dietary *Bos taurus* (bta)-specific (pre-) miRNAs as tracers. The 50 top-ranked bovid-specific pre-mir were used for heat map illustration (specimens: 8 cattle, 1 yak, 1 water buffalo) (Figure 1E; left column). Further, 11 formula/powdered milk products are shown (compare Table S3A) (Figure 1E; right column). Most bovid-specific pre-mir from liquid milk were present in formula products with similar relative quantities, but mostly with lower total miRNA concentrations in formula (Figure 1F).



For deeper investigation of their putative influence in a human host we selected several bta-miRs using relative quantities and the validated the absence of similar miRs in the human miRNome as the main selection criteria (Figure 1E, red font). Selected bta-miRNA quantities were estimated via their ranks (#n) within *Bos taurus* total miRNAs: bta-mir-2904 (#19); bta-mir-2887 (#67); bta-mir-2478 (#93); bta-mir-3533 (#141); bta-mir-2428 (#169); bta-mir-2440 (#172); bta-mir-677 (#191); bta-mir-2892 (#229); bta-mir-2404 (#232); bta-mir-2361 (#237); bta-mir-2372 (#278); bta-mir-2304 (#284). Typically, human mRNA target prediction for those bta-miRNAs via miRDB (26) revealed dozens of potential high scoring 3'-UTR targets, with transcripts of several master regulatory genes among them (Table S4). For example, for bta-miR-677-5p (5'-CUCACUGAUGAGCAGCUUCUGAC-3', probable seed-sequence underlined), transcription factor SP4, *zink finger and homeobox family member 1* (ZHX1) and the chromatin remodeller ATRX were among the predicted human mRNA targets (n=655). Importantly, such algorithms usually deliver large numbers of false-positive results, which might be invalid for specific cell types-of-interest. But before interrogating this problem, it is crucial to address whether (xenobiotic) miRNAs stay intact during the gastric and intestinal transit and eventually do reach potential mRNA targets within cells.

#### *Dietary-derived bta-miRs survive gastrointestinal transit in human newborns*

Consistently, we examined a randomly selected preterm neonate stool sample collection from an intensive care neonatology unit. The donors were given routinely formula supplementation (mean gestational age: 29.2 wks [24.4-35.7]) (27). Quantitative real-time PCR (qPCR) analyses were performed using cDNA libraries prepared from purified small RNAs and specific sets of bta-miR or pan-miR primer pairs (Table S3B). As a matter of fact, we detected intact all interrogated bta-miRs in all pre-term stool samples (Figure 2A). This demonstrates that nutritional uptake of milk miRNAs leads to their intestinal enrichment and suggests their stable sequence integrity during gastrointestinal (GI) transit in human preterm neonates.

#### *Xenobiotic miRNAs become enriched in preterm piglets' intestinal cells following 9-days enteral nutrition with bovine colostrum or formula*

We studied intestinal cellular uptake of milk miRNAs in vivo exploiting bovine colostrum or formula derived bta-miRs as tracers in a preterm neonate piglet model wherein the effects of enteral feeding introduction post-delivery are subject of comprehensive ongoing studies (8-12). Following 9 days of bovine colostrum or formula supplementation after the introducing enteral feeding a protocol for intestinal epithelial cell enrichment was applied prior to miRNA library preparation and deep sequencing. Strikingly, we found 4 bta-miRs, which became enriched within the 50 top-ranked intestinal cellular miRNAs (Figure 3A). Thereby, bta-miR-2904 occupied rank #4 suggesting that a dietary miRNA could in principle reach biologically significant levels if being taken up by cells. Apparently, the rate of cellular uptake was partly influenced by the bta-miR abundance in bovine milk (bta-miR-2904: #4 in intestinal cells (IC) vs. #1 (bta-specific miRs) in bovine milk (BM); bta-miR-2881: #31/not ranked in IC/BM; bta-miR-2892: #37/6 in IC/BM; bta-miR-2887: #39/2 in IC/BM; compare Figure 1E). Apart, we note that for the many miRNAs with identical sequences in different taxa an endogenous or food-derived origin might be impossible to discriminate.

*In neonatal preterm piglets feeding with cel-miR-39-5p/-3p-supplemented colostrum bolus leads to bloodstream enrichment of reporter miRNAs*

Following the observation that 9-days-feeding leads to xenobiotic miR enrichment in intestinal cells of neonate piglets, we interrogated whether milk miRNAs could possibly also be involved as regulators in the development of gut homeostasis or other developmental processes, which start perinatally or early postnatally. Therefore, we studied whether and how fast dietary colostrum bolus supplementation with reporter miRNAs (cel-miR-39-5p and cel-miR-39-3p [Figure 3B]) can lead to bloodstream accumulation of xenobiotic cel-miR tracers after GI transit utilizing the preterm piglet model. At different time points post-feeding ( $t_1=30$  min,  $t_2=1$  h,  $t_3=2$  h,  $t_4=3$  h,  $t_5=5$  h and  $t_6=7$  h) peripheral blood was sampled. Then total serum RNA was used for miRNA library preparation and successive analyses of enrichment of both reporter cel-miRNAs by qPCR. MicroRNA-seq was conducted from serum sampled 7 h post-feeding for confirmation. Along most time points of sampling, we did not observe qPCR signals above threshold, but 7 h post feeding the signal for cel-miR-39-3p massively increased (Figure 3B) suggesting the transit of considerable amounts of cel-

miR-39-3p from the GI tract into the bloodstream. At this timepoint enrichment was not observed for cel-miR-39-5p. Reads for cel-miR-39-3p could be verified by miRNA-seq, which was reminiscent of the cel-miR-39-3p/5p-bias observed in qPCR analyses before (Figure 3C), but reasons remain unclear. Remarkably, the timing of reporter miRNA accumulation in serum very roughly appeared to be in agreement with GI transit times of radiotracers in suckling piglets (21 days old; approx. 1.5-3.5 h until 75% of gastric emptying and >9.5 h until 75% intestinal emptying) (28).

#### *Dietary supplemented cel-miR-39-5p and cel-miR-39-3p co-precipitate with Ago2*

The biological activity of miRNAs requires their loading into Ago2-containing protein complexes. We analysed whether cel-miR-39-5p/-3p miRNAs can be pulled-down from piglet intestinal biopsies 7h post-feeding using the anti-pan-Ago2 monoclonal antibody (Sigma-Aldrich, MABE56, clone 2A8). Both cel-miR-39-5p as well as cel-miR-39-3p could be detected in Ago2-precipitates from pre-term piglets, which were fed with reporter-miRNA-supplemented colostrum, suggesting that Ago2 in intestinal cells can be loaded with both the guide and the passenger strands resulting from processed cel-mir-39 (Figure 3D). Remarkably, the stronger signal for cel-miR-39-3p was reminiscent of its predominant enrichment in the bloodstream 7h post-feeding. Due to the presence of positive cel-miR-39-5p qPCR signals in Ago2-immunocomplexes we assume that its bloodstream enrichment could simply lag behind cel-miR-39-3p instead of being selectively excluded.

#### *Weak evidence for DDX3 targeting through bta-mir-677 in HIEC-6 cells is superimposed by several probable false-positive predictions of miRNA-mRNA interactions*

If anticipating a vertical transmission of PTGS via milk miRNAs, the superordinate problem is which mRNAs are true targets. Clearly, target prediction depending mostly of 5'-seed complementarity remains leaky for simple reasons: First, because searches for sequence matches in mRNA databases usually cannot consider whether a potential target is transcribed in a cell or tissue-of-interest or not. Second, prediction algorithms do not consider that within a cell different miRNAs and mRNAs compete for being loaded to a limited number of Argonaute (Ago) proteins (29). Moreover, given that mRNA decay and blocking of translation exist as alternative miRNA interference mechanisms, it is

not clear whether PTGS can be detectable directly on the mRNA level and/or the protein level only. Consequently, the identification of valid miRNA-target interactions and their influence on gene regulatory networks requires detailed experimental analyses.

We thus studied the potential influence of bta-mir-677 on bioinformatically predicted human targets in primary foetal human intestinal epithelial cells (HIEC-6) using adenovirus type 5 (Ad5)-based miRNA gene transfer. Using this transduction method, we efficiently overcame the disadvantageous signal-to-noise ratio of standard transfection protocols (Figure S3). Transcriptome profiling confirmed that this model well fulfilled important criteria for the purpose of miRNA experiments in non-transformed cells, which retained foetal epithelial cell characteristics under primary cell culture conditions and under the influence of Ad5-mediated miRNA transfer (Figure 4A). From the list of predicted human mRNA targets of bta-miR-677-5p, we selected ATRX, DDX3, PLCXD3 and ZHX1 for analyses by immunofluorescence microscopy and quantitative Western blots (Figure 4B,C). These targets had a high miRDB scores, and they were annotated being potential master regulatory genes. However, from this unavoidably arbitrarily selection, none of the candidates exhibited differences in the quantity or subcellular distribution using microscopy (Figure 4B). On the scale of whole cell populations, we conducted quantitative Western blot analyses. Interestingly, for DDX3, analyses of two Western blots revealed a 24.45% reduction (SD:  $\pm 1.68\%$ ) of DDX3 signals in bta-mir-677-treated vs. wild-type and a 37.90% (SD:  $\pm 1.90\%$ ) DDX3 signal reduction in bta-mir-treated vs. ctrl-mir-treated HIEC-6. These results suggested that bta-mir-677 expression in HIEC-6 cells could indeed influence the expression of one of the predicted human mRNA targets, leading to reduced translated DDX3 protein. Even though the latter observation could give some hint for an influence of bta-miR-677-5p in HIEC-6 cells, the relative arbitrary putative target selection and laborious validation is unrewarding and non-holistic. We therefore analysed the influence of Ad5-mediated miRNA gene transfer using four different bovine miRNAs-of-interest (miRoI) (bta-miR-677-5p, bta-miR-2404-5p, bta-miR-2440-3p and bta-miR-2361). We determined the fold-changes of all transcribed genes in miRoI-treated cells with reference to non-sense miR-treated HIEC-6. For comparison, we then focussed our analyses on all expressed predicted target genes of each miRoI with reference to non-sense miR-treated HIEC-6 (Figure 4D). Whereas most genes remained unaffected by miRoI-treatment, we observed numerous

significant cases of downregulation within the group of predicted miRoI targets (Median fold-changes all transcripts/predicted targets: bta-miR-677-5p: 0.9908/0.8147 [ $p < 0.0001$ ]; bta-miR-2404-5p: 0.9805/0.9587 [ $p = 0.0032$ ]; bta-miR-2440-3p: 1.0070/0.9728 [ $p = 0.0240$ ]; bta-miR-2361-5p: 1.0340/0.9361 [ $p < 0.0001$ ]), whereby we did not see any correlation between the degree of observed downregulation and the individual position/score as a result of target predictions.

## Conclusion

Taken together, our experimental trajectory suggests that dietary uptake of milk miRNAs can lead to their loading to Ago2 in neonatal intestinal epithelial cells. Thus, vertical transmission of maternal milk miRNA signals via GI transit to responsive cells and systemic bloodstream distribution is apparently possible. This is in agreement with the ‘functional hypothesis’, but contradicts the ‘non-functional’ hypothesis that milk miRNAs could solely serve as a nucleoside source for the newborn (30). Our results from tracer experiments provide good experimental justification to address superordinate questions about milk miRNA-induced PTGS in neonates. However, key problems remain and should be addressed: We have no idea, which of the hundreds of different miRNAs found in milk with different abundance could be important and how selective loading of Ago2 in milk miRNA-responsive cells could work. Possibly, only some specific miRNAs find specific mRNA duplex partners, depending on their presence in specific cell types and transcriptional timing. Systemically, it remains unknown how far-reaching milk miRNAs’ influence could be. Could biologically relevant miRNA accumulation be restricted to the intestine, or does their observation in the bloodstream indicate a systemic distribution to other target tissues/cells? As important as the place of milk miRNA activity is the time of action during ontogeny. Most convincing could be the existence of a relatively narrow ‘window of opportunity’, which could open perinatally and could persist during the introduction of enteral feeding, when the infant’s intestine develops as an environment-organism interface to coordinate microbiome homeostasis.

In HIEC-6, we have efficiently applied Ad5-mediated gene transfer, establishing continuous, but probably non-natural cellular levels of ectopically expressed miRNAs. This might lead to enforced

Ago2-loading caused by outnumbered availability of the substrate (dog-eat-dog effect). These conditions may not fully reflect the in vivo situation in the neonate intestine, but nevertheless might be useful to study the influence of (xenobiotic) milk miRNAs on gene regulatory networks. This approach could plausibly help to explain the observed increase of severe intestinal complications such as NEC in premature infants fed with bovine based formula milk. However, we clearly emphasize that postulating potential harmful influence would be an overstated conclusion from our experiments. But for the first time in human history, the newest developments in intensive care neonatology allow the survival of extremely vulnerable preterm neonates, whereby severe complication are often associated with incomplete intestinal development. Thus, if the ‘window of opportunity’ hypothesis discussed above holds, the consideration of xenobiotic milk miRNA side effects on early preterm and term neonatal development seems well justified and would encourage advanced future studies.

## **Methods**

### Samples and animal procedures

Human milk and stool specimens were collected with approval of the Witten/Herdecke University Ethics board (No. 41/2018) after informed written consent was obtained by all involved donors.

Animal milk was purchased or collected with the help of Wuppertal Zoo, local farmers or veterinary medics. All animal procedures were approved by the National Council on Animal Experimentation in Denmark (protocol number 2012-15-293400193). Piglet (landrace × large white × duroc; delivered by caesarean section on day 105 [90%] of gestation) blood and gut biopsies derived from an experimental ongoing series described previously (8).

For reporter microRNA supplementation of bovine colostrum bolus for piglet feeding reported milk nucleic acids concentration were used as guideline (23 mg/L ± 19 mg/L [8.6-71 mg/L]) (31). We supplemented bovine colostrum bolus with RNA oligonucleotides mimicking both putatively processed strands of *Caenorhabditis elegans* (cel), cel-miR-39-5p and cel-miR-39-3p (Figure 3B), and adjusted their amount to achieve approx. 5-10% of human milk’s total nucleic acids content. Three neonatal low-birth-weight piglets from the same litter (mean birth weight 1,119 g [1,071-1,167 g];

normal birth weight approx. 1,400-1,500 g) received initial feeding ( $t_0$ ) of bovine colostrum bolus (15 mL/kg) enriched with 39 g/L casein glycomacropeptide (CGMP), 2.8 g/L osteopontin (OPN) and a mix of cel-miR-39-5p/-3p reporter microRNAs. As control, three other piglets from the same litter received colostrum bolus without reporter microRNA supplementation (mean birth weight 1,047 g [862-1,240 g]). After 2.5 h, the piglets received another bolus to facilitate gut motility. At different time points post-feeding ( $t_1=30$  min,  $t_2=1$  h,  $t_3=2$  h,  $t_4=3$  h,  $t_5=5$  h and  $t_6=7$  h) 1 mL peripheral blood was sampled. Total RNA was used for microRNA library preparation and successive analyses of enrichment of both reporter cel-microRNAs by qPCR, whereas confirmatory microRNA-seq was conducted 7 h post-feeding only.

Enrichment of piglet intestinal epithelial cells from intestinal mucosa biopsies was done as follows. Pigs were euthanised using 200 mg/kg intraarterial sodium pentobarbital after anaesthesia administration. The GI tract was immediately removed, and the small intestine was carefully emptied of its contents. 30 cm of the distal small intestine were used for cell collection. The segment was flushed with 10 mL of pre-chilled NaCl 0.9% (Fresenius Kabi, Uppsala, Sweden) and then cut open along the length. The upper layer of the intestinal mucosa was gently scraped off with a microscopic slide and transferred in a 15 mL tube containing 12.5 mL PBS containing FBS (final concentration 1.12  $\mu$ L/mL). Homogenization was achieved by pipetting with a plastic Pasteur pipette for about 1 min and then stirring the solution at 500 rpm for 20 min at room temperature. The homogenized suspension was filtered through a 70  $\mu$ m cell sieve and spun down at 500 xg at 4°C for 3 min. The cell pellet was resuspended in 5 mL modified PBS (see above), filtered and centrifuged again. The pellet was then resuspended in 1 mL red blood cell lysis buffer (1x, Invitrogen™, ThermoFisher Scientific), incubated for 5 min at room temperature and then spun down at 500 xg at 4°C for 3 min. The cell pellet was washed again and finally resuspended in 1 mL modified PBS (see above). From the resulting single cell suspension 250  $\mu$ L were used for RNA purification. The authors state that they have obtained appropriate institutional review board approval or have followed the principles outlined in the Declaration of Helsinki for all human or animal experimental investigations.

### Nucleic acids

Total RNA was purified from milk serum, blood serum, radically grinded tissue, cells and stool samples using Trizol reagent (Sigma, MO, USA) upon manufacturer's recommendations. RNA quality and quantity were assessed by microcapillary electrophoresis using an Agilent Bioanalyzer 2100 similarly as described (32). A list of oligonucleotides used is provided as appendix (Table S3A).

### Real time PCR

Quantitative measurement of microRNAs was analysed from cDNA libraries (as described in (32)) using primer pairs as listed (Table S3A) and the QuantiTect SYBR Green PCR Kit (Qiagen) using a Corbett Rotor-Gene 6000 qPCR machine. Specifically, a combination of miR-specific forward primers [bta/pan-miR-*name*-5p/-3p-fw] and library-specific reverse primers [library\_P*n*\_miR\_rv]) was used (Table S3B). PCR conditions were as follows: 95°C for 15 min, 40 cycles of (95°C for 15 s, 60°C for 30 s). Amplicon melting was performed using a temperature gradient from 55–95°C, rising in 0.5°C increments. For relative comparative quantification of quantitative expression fold changes we utilized the  $\Delta\Delta C_t$  method (33) using stable miR-143-3p, miR-99b-5p and let7b-5p for normalization.

### Deep sequencing of miRNAs (miRNA-seq) and bioinformatics pipeline

Small RNAs (18-36 nt) were purified from total RNA using polyacrylamide gel electrophoresis (PAGE). The subsequent cDNA library preparation utilizes a four-step process starting with the ligation of a DNA oligonucleotide to the 3'-end of the selected small RNAs, followed by ligation of a RNA oligonucleotide to the 5'-end of the selected small RNAs. The resulting molecules were transcribed via reverse transcription (RT) and amplified via PCR (32). Subsequently, after final quality checks by microcapillary electrophoresis and qPCR, the libraries were sequenced on an Illumina HiSeq 2000 platform (single end, 50 bp). This work has benefited from the facilities and expertise of the high throughput sequencing core facility of I2BC (Research Center of GIF – <http://www.i2bc.paris-saclay.fr/>). The initial data analysis pipeline was as follows: CASAVA-1.8.2 was used for demultiplexing, Fastqc 0.10.1 for read quality assessment and Cutadapt-1.3 for adaptor trimming, resulting in sequencing reads and the corresponding base-call qualities as FASTQ files. File



conversions, filtering and sorting as well as mapping, were done using ‘Galaxy’ (34-36), a platform for data intensive biomedical research (<https://usegalaxy.org/>), or ‘Chimira’ (37), sRNAtoolbox (38) or ‘miRBase’ (25), respectively. For selected bta-mir we used the miRDB custom option for sequence-based prediction of potential human mRNA targets (26).

#### Argonaute co-immunoprecipitation (Co-IP)

Association of reporter cel-miR-39 co-fed with milk with Argonaute (Ago2) in piglet intestinal biopsies was analysed using co-immunoprecipitation and qPCR. For native pan-Ago2 precipitation from intestinal tissue we used monoclonal mouse anti-pan-Ago2 antibodies (Sigma-Aldrich, MABE56, clone 2A8) similarly as described previously (39). This antibody exhibits cross-species reactivity with Ago2 from mouse, humans, and most probably from other mammals as well. After final blood sampling 7-7.5 h post-feeding proximal and distal tissues were taken at euthanasia, deep frozen at -20°C and shipped on dry ice. Prior to immunoprecipitation piglet intestinal tissue from a liquid nitrogen storage tank was powdered using a Cellcrusher™ (Cellcrusher, Co. Cork, Ireland) pre-chilled in liquid nitrogen. Subsequently, intestinal tissue powder was suspended in lysis buffer (20 mM Tris-HCl, pH7.5, 200 mM NaCl, 2.5 mM MgCl<sub>2</sub>, 0.5% Triton X-100). Samples were incubated overnight with 3 µg anti-pan-Ago (2A8) and 25 µL magnetic protein A beads (Diagenode). Following the enrichment of immunocomplexes on a magnetic rack and several washes with PBS, the samples were heated to 95°C for 15 min, and then RNA was purified from the immunocomplexes using Trizol and isopropanol precipitation. Then RNA converted into cDNA libraries and cel-miR-39-5p/-3p were analysed from cDNA libraries by qPCR.

#### Deep sequencing of miRNAs (miRNA-seq) and bioinformatics pipeline

Small RNAs (18-36 nt) were purified from total RNA using polyacrylamide gel electrophoresis (PAGE). The subsequent cDNA library preparation utilizes a four-step process starting with the ligation of a DNA oligonucleotide to the 3’-end of the selected small RNAs, followed by ligation of a RNA oligonucleotide to the 5’-end of the selected small RNAs. The resulting molecules were transcribed via reverse transcription (RT) and amplified via PCR (32). Subsequently, after final quality

checks by microcapillary electrophoresis and qPCR, the libraries were sequenced on an Illumina HiSeq 2000 platform (single end, 50 bp). This work has benefited from the facilities and expertise of the high throughput sequencing core facility of I2BC (Research Center of GIF – <http://www.i2bc.paris-saclay.fr/>). The initial data analysis pipeline was as follows: CASAVA-1.8.2 was used for demultiplexing, Fastqc 0.10.1 for read quality assessment and Cutadapt-1.3 for adaptor trimming, resulting in sequencing reads and the corresponding base-call qualities as FASTQ files. File conversions, filtering and sorting as well as mapping, were done using ‘Galaxy’ (34-36), a platform for data intensive biomedical research (<https://usegalaxy.org/>), or ‘Chimira’ (37), sRNAtoolbox (38) or ‘miRBase’ (25), respectively. For selected bta-mir we used the miRDB custom option for sequence-based prediction of potential human mRNA targets (26).

### Luciferase assay

A SacI/NheI fragment with sticky ends was hybridized from oligonucleotides through incubation in a boiling water bath and successive chilling to room temperature (Table S3B). We cloned this fragment containing a 7bp motif reverse complementary to the 5’-seed (nucleotides 2-8; 5’-ucacuga-3’) of bta-miR-677-5p into the 3’-UTR region of the firefly luciferase gene (*luc2*) encoded in the pmirGLO dual luciferase expression vector (Promega) (Figure 2B). For bioluminescence calibration this vector contains another luciferase cassette (*Renilla*; hRluc-neo fusion). Subsequently, pmirGLO was co-transfected with bta-mir-677-like hairpin RNAs or non-luciferase directed controls, respectively, into HeLa cells using Lipofectamin 2000 (ThermoFisher) transfection reagent upon manufacturer’s recommendations, prior to bioluminescence quantification using a GloMax® Multi Detection System (Promega). We performed this experiment to rule out exemplarily that the observed bta-miR-candidates could be simply microRNA-like sequence artefacts without any function, we interrogated whether bta-miR-677, a candidate microRNA with intermediate abundance in milk can silence luciferase expression *in vitro* via a predicted 3’-UTR target sequence in a human HeLa cell-based assay. Therefore, we cloned a SacI/NheI fragment containing a 7 bp 3’-UTR target motif reverse complementary to the 5’-seed (nucleotides 2-8) of bta-miR-677-5p into the 3’-UTR region of the firefly luciferase gene (*luc2*) encoded in the pmirGLO dual luciferase expression vector (Promega)

(Figure S4A). For bioluminescence calibration this vector contained a 2<sup>nd</sup> luciferase cassette (*Renilla*; hRluc-neo fusion). Subsequently, pmirGLO was co-transfected with bta-mir-677-like hairpin RNAs or non-luciferase directed controls, followed by bioluminescence quantification. We observed very robust silencing of firefly luciferase upon bta-mir-677-like co-transfection, suggesting that at least bta-miR-677-5p can function as valid microRNA in human cells (Figure S4B).

#### Insertion of microRNA hairpins into Ad5 vectors

To assess the effects of microRNA overexpression in cell culture Ad5-based replication deficient  $\Delta$ E1 vectors harbouring an hCMV promoter-driven expression cassette for the concomitant expression of EGFP (as transduction marker) and microRNAs were generated based on the 'BLOCK-iT Pol II miR RNAi Expression Vector Kits' protocol (Invitrogen). Vectors were serially amplified on 293 cells and purified by CsCl density centrifugation. The vector titers were determined by OD260 and vector genome integrity was confirmed by sequencing and restriction digest analysis (40). Hairpins mimicking bovine pre-mirs were designed to express microRNAs, which corresponded to bta-miR-677-5p, bta-miR-2404-5p, bta-miR-2440-3p, bta-miR-2361-5p. Details of vector design can be obtained upon request. The expression of bta-mir-677-like hairpins, bta-miR-677-5p and bta miR-677-3p, respectively, was evaluated by qPCR using the Mir-X™ miRNA First Strand Synthesis Kit (Takara).

#### Cell culture and Ad5 transduction

Human intestinal epithelial cells (HIEC-6 [ATCC CRL-3266]) cells were cultured upon manufacturer's recommendations. Flow cytometric analyses of HIEC-6 cells transduced with different ranges of multiplicity of infection (MOI) were used to define a transduction efficiency and to determine the optimal MOI (Figure S3). Considering transduction efficiency and compatibility, we subsequently used MOI 10.000 in experimental routine. One day pre-transduction, 10<sup>6</sup> HIEC-6 cells were seeded in 6-well cell culture dishes. The following day, cells were washed with PBS, provided with fresh medium and subsequently transduced with respective Ad5 vector particles. Cells were harvested 96 h post-transduction. The expression of bta-mir-677-like hairpins, bta-miR-677-5p and

bta-miR-677-3p, respectively, was validated using the Mir-X™ miRNA First Strand Synthesis Kit (Takara) in combination with qPCR. The results confirmed the expression of bta-mir-677-like hairpins, bta-miR-677-5p, but a bias for bta-miR-677-3p suggesting preferential processing of the 5-p guide strand (Figure S5). For Western blot analyses cell pellets were homogenized in RIPA buffer (50 mM Tris HCl pH 8.0, 150 mM NaCl, 1% NP-40, 0,5% sodium deoxycholate, 0,1% SDS plus cOmplete™ Mini Protease Inhibitor Cocktail [Sigma-Aldrich]). Alternatively, cells were grown on coverslips for immunofluorescence microscopy. Here, after Ad5-mediated miRNA transfer successful expression of the miRNA transgene could be indirectly confirmed using immunofluorescence microscopy and flow cytometry for detection of green fluorescent protein (GFP) that was co-expressed with bta-mir-677-like hairpins from the same transcript.

#### Western blot analyses

Homogenized pellets were mixed with SDS. Proteins were separated by SDS-PAGE using 5% stocking and 8% running gels and subsequently transferred to a nitrocellulose blotting membrane (Amersham Protran Premium 0.45 µm NC). Membranes were blocked 1% BSA in TBST (20 mM Tris; 150 mM NaCl; 0.1% Tween 20; pH 7.4). Polyclonal rabbit anti-ATRX (Abcam; ab97508), polyclonal rabbit anti-DDX3 (Abcam; ab235940), polyclonal rabbit anti-ZHX1 (Abcam; ab19356), polyclonal rabbit anti-PLCXD3 (Sigma-Aldrich; HPA046849), polyclonal rabbit anti-GAPDH (Sigma-Aldrich; G8795) were used as primary antibodies at 1:500 dilution in blocking buffer, except anti-GAPDH (dilution 1:20,000 in blocking buffer). For internal normalization anti-GAPDH was used in parallel and simultaneously with each other primary antibody. Secondary antibodies were goat anti-rabbit IRDye 800CW (LI-COR; 926-32211) and goat anti-mouse IRDye 680RD (LI-COR; 926-68070), each being diluted 1:10,000 as a mix in blocking buffer. Fluorescence was monitored using the Odyssey CLx Imaging system (LI-COR) with the 2-color detection option and analysed using Image Studio software (LI-COR).

### Immunofluorescence microscopy

5x 10<sup>5</sup> HIEC-6 cells were grown on coverslips in 6-well plates and transduced as described above. 96 h post-transduction cells were fixed for 10 min in 2% PFA/DPBS, washed twice with DPBS and then permeabilised using 0.5% Triton X-100/DPBS, followed by 0.1N HCl for exactly 5 min for antigen retrieval and successive washes with DPBS. Blocking was done in 3% BSA/0.1% Triton X100/DPBS. Subsequently, the primary antibodies were incubated in blocking buffer for 1 h/37°C: 1. polyclonal rabbit anti-ATRX (Abcam; ab97508) at 1:100, polyclonal rabbit anti-DDX3 (Abcam; ab235940) at 1:500, polyclonal mouse anti-ZHX1 (Abcam; ab168522) at 1:100. Then polyclonal goat anti-rabbit Cy3 (Jackson ImmunoResearch) or polyclonal goat anti-mouse Cy3 (Jackson ImmunoResearch) were used as secondary antibodies, each at 1:100. Eventually, 4',6-diamidino-2-phenylindole (DAPI) was used for DNA counterstaining at 0.1 µg/mL followed by washes and mounting with Prolong Gold (Invitrogen). Acquisition of images was done with a Nikon Eclipse Ti Series microscope. Fluorochrome image series were acquired sequentially generating 8-bit grayscale images. The 8-bit grayscale single channel images were overlaid to an RGB image assigning a false color to each channel using open source software ImageJ (NIH Image, U.S. National Institutes of Health, Bethesda, Maryland, USA, <https://imagej.nih.gov/ij/>).

### Deep sequencing of messenger RNAs (mRNA-seq) and bioinformatics pipeline

Total RNA was purified from Ad5-transduced HIEC-6 cells expressing a nonsense-miR or bta-miRs using Trizol reagent (Sigma, MO, USA) upon manufacturer's recommendations. RNA quality and quantity were assessed by microcapillary electrophoresis using an Agilent Bioanalyzer 2100. All specimens had a RIN between 8.9 and 9.2 and were subsequently used for sequencing library preparation. Enrichment of mRNAs was done using the NEBNext Poly(A) mRNA Magnetic Isolation Module (New England BioLabs, #E7490S) upon manufacturers' recommendations. Subsequently cDNA libraries were prepared using the NEBNext Ultra II DNA Library Prep Kit for Illumina (New England BioLabs, #E7645S) upon manufacturers' recommendations in combination with NEBNext Multiplex Oligos for Illumina (Index Primer Set 1) (New England BioLabs, #E7335G). Before multiplexing, library quality and quantity were assessed by microcapillary electrophoresis using an

Agilent Bioanalyzer 2100. Deep sequencing was done using an Illumina HiSeq2500. The initial data analysis pipeline was as follows: CASAVA-1.8.2 was used for demultiplexing, Fastqc 0.10.1 for read quality assessment and Cutadapt-1.3 for adaptor trimming, resulting in sequencing reads and the corresponding base-call qualities as FASTQ files. File conversions, filtering and sorting as well as mapping, were done using 'Galaxy' (34-36) (<https://usegalaxy.org/>), serially shepherding the FASTQ files through the following pipeline of tools: 1. FASTQ groomer (Input: Sanger & Illumina 1.8+ FASTQ quality score type) (41); 2. TopHat for gapped-read mapping of RNA-seq data using the short read aligner Bowtie2 (Options: single end, Homo sapiens: hg38) resulting in a BAM formatted accepted hits file (42). 3. featureCounts to create tabular text file (Output format: Gene-ID "\t" read-count [MultiQC/DESeq2/edgeR/limma-voom compatible]). 4. Prior to DESeq2 normalization, a tabular file containing catalogued columns of read counts for all experiments was arranged in Microsoft Excel for Mac 16.32. and then uploaded as a tabular text file to Galaxy. 5. annotadeMyIDs was used to assign gene symbols and gene names to Entrez IDs. Biostatistical tests were carried out using GraphPad Prism 8.4.3 software.

### Statement

All authors had access to the study data and had reviewed and approved the final manuscript.

### Availability of data and materials

The datasets generated and/or analysed during the current study are available in the NCBI BioProject repository as fastq.gz files of miRNA-seq and mRNA-seq (SubmissionIDs: SUB7584111/SUB9897357/BioProject ID: PRJNA740153/URL: <https://www.ncbi.nlm.nih.gov/bioproject/740153>).

### **Declarations**

#### **Ethics approval and consent to participate**

This study was conducted with approval of the Witten/Herdecke University Ethics board (No. 41/2018). All animal procedures were approved by the National Council on Animal Experimentation

in Denmark (protocol number 2012-15-293400193). The authors state that they have obtained appropriate institutional review board approval or have followed the principles outlined in the Declaration of Helsinki for all human or animal experimental investigations. In addition, for investigations involving human subjects, informed consent has been obtained from all participants. Patients or the public were not involved in the design, or conduct, or reporting, or dissemination plans of our research

### **Authors' contributions**

JP and PPW designed the study and wrote the paper. SR conducted Ad5-mediated miRNA gene transfer experiments under supervision and with the help of FK, FJ and CH. Further, she prepared mRNA-seq libraries. FK and JS developed the Ad5-mediated miRNA gene transfer. CAH traced miRNAs in piglet blood and intestine and human stool. MA, AP and VO performed luciferase experiments. Animal treatments as well as sample collection and preparation were done by DNN, PPJ and PTS. PPW, FG, TT, MA, ACWJ and SW contributed to sampling of human and animal milk specimens. PPW, FG, VW and CAH generated RNA libraries, conducted qPCR experiments and NGS. JP and CAH performed Argonaute pull-down experiments. JP and PPW supervised undergraduates and graduate students. JP supervised the study, analysed the data and wrote the manuscript with the help of PPW, ACWJ, CH and FK.

### **Acknowledgements**

We gratefully acknowledge Gilles Gasparoni (Institut für Genetik/Epigenetik, Universität des Saarlandes, Germany) to enable and support our mRNA deep sequencing analyses under hard conditions during the first European peak period of the SARS-CoV-2 pandemic. We further thank Dr. Arne Lawrenz (director of Wuppertal Zoo) for providing Okapi (Lomela's) milk.

## References

1. Brandt G, Szecsenyi-Nagy A, Roth C, Alt KW, Haak W. Human paleogenetics of Europe--the known knowns and the known unknowns. *J Hum Evol* 2015;79:73-92.
2. Gerbault P. The onset of lactase persistence in Europe. *Hum Hered* 2013;76:154-161.
3. Segurel L, Bon C. On the Evolution of Lactase Persistence in Humans. *Annu Rev Genomics Hum Genet* 2017;18:297-319.
4. Beja-Pereira A, Luikart G, England PR, Bradley DG, Jann OC, Bertorelle G, Chamberlain AT, et al. Gene-culture coevolution between cattle milk protein genes and human lactase genes. *Nat Genet* 2003;35:311-313.
5. Gerbault P, Liebert A, Itan Y, Powell A, Currat M, Burger J, Swallow DM, et al. Evolution of lactase persistence: an example of human niche construction. *Philos Trans R Soc Lond B Biol Sci* 2011;366:863-877.
6. Nuñez M: Existing Technologies in Non-cow Milk Processing and Traditional Non-cow Milk Products. In: Tsakalidou E, Papadimitriou K, eds. *Non-Bovine Milk and Milk Products*: Academic Press, 2016; 161-185.
7. Shulman RJ, Schanler RJ, Lau C, Heitkemper M, Ou CN, Smith EO. Early feeding, feeding tolerance, and lactase activity in preterm infants. *J Pediatr* 1998;133:645-649.
8. Willems R, Krych L, Rybicki V, Jiang P, Sangild PT, Shen RL, Hensel KO, et al. Introducing enteral feeding induces intestinal subclinical inflammation and respective chromatin changes in preterm pigs. *Epigenomics* 2015;7:553-565.
9. Bjornvad CR, Schmidt M, Petersen YM, Jensen SK, Offenberg H, Elnif J, Sangild PT. Preterm birth makes the immature intestine sensitive to feeding-induced intestinal atrophy. *Am J Physiol Regul Integr Comp Physiol* 2005;289:R1212-1222.
10. Lin PW, Stoll BJ. Necrotising enterocolitis. *Lancet* 2006;368:1271-1283.



11. Moller HK, Thymann T, Fink LN, Frokiaer H, Kvistgaard AS, Sangild PT. Bovine colostrum is superior to enriched formulas in stimulating intestinal function and necrotising enterocolitis resistance in preterm pigs. *Br J Nutr* 2011;105:44-53.
12. Sangild PT, Siggers RH, Schmidt M, Elnif J, Bjornvad CR, Thymann T, Grondahl ML, et al. Diet- and colonization-dependent intestinal dysfunction predisposes to necrotizing enterocolitis in preterm pigs. *Gastroenterology* 2006;130:1776-1792.
13. Bartel DP. MicroRNAs: target recognition and regulatory functions. *Cell* 2009;136:215-233.
14. Brennecke J, Stark A, Russell RB, Cohen SM. Principles of microRNA-target recognition. *PLoS Biol* 2005;3:e85.
15. Chipman LB, Pasquinelli AE. miRNA Targeting: Growing beyond the Seed. *Trends Genet* 2019;35:215-222.
16. Djuranovic S, Nahvi A, Green R. A parsimonious model for gene regulation by miRNAs. *Science* 2011;331:550-553.
17. Weber JA, Baxter DH, Zhang S, Huang DY, Huang KH, Lee MJ, Galas DJ, et al. The microRNA spectrum in 12 body fluids. *Clin Chem* 2010;56:1733-1741.
18. Chen X, Gao C, Li H, Huang L, Sun Q, Dong Y, Tian C, et al. Identification and characterization of microRNAs in raw milk during different periods of lactation, commercial fluid, and powdered milk products. *Cell Res* 2010;20:1128-1137.
19. Melnik BC. Milk: an epigenetic amplifier of FTO-mediated transcription? Implications for Western diseases. *J Transl Med* 2015;13:385.
20. Melnik BC. Milk disrupts p53 and DNMT1, the guardians of the genome: implications for acne vulgaris and prostate cancer. *Nutr Metab (Lond)* 2017;14:55.
21. Melnik BC, Schmitz G. Milk's Role as an Epigenetic Regulator in Health and Disease. *Diseases* 2017;5.

22. Title AC, Denzler R, Stoffel M. Uptake and Function Studies of Maternal Milk-derived MicroRNAs. *J Biol Chem* 2015;290:23680-23691.
23. Kahn S, Liao Y, Du X, Xu W, Li J, Lonnerdal B. Exosomal MicroRNAs in Milk from Mothers Delivering Preterm Infants Survive in Vitro Digestion and Are Taken Up by Human Intestinal Cells. *Mol Nutr Food Res* 2018;62:e1701050.
24. Perge P, Nagy Z, Decmann A, Igaz I, Igaz P. Potential relevance of microRNAs in inter-species epigenetic communication, and implications for disease pathogenesis. *RNA Biol* 2017;14:391-401.
25. Griffiths-Jones S, Grocock RJ, van Dongen S, Bateman A, Enright AJ. miRBase: microRNA sequences, targets and gene nomenclature. *Nucleic Acids Res* 2006;34:D140-144.
26. Chen Y, Wang X. miRDB: an online database for prediction of functional microRNA targets. *Nucleic Acids Res* 2020;48:D127-D131.
27. Zoppelli L, Guttel C, Bittrich HJ, Andree C, Wirth S, Jenke A. Fecal calprotectin concentrations in premature infants have a lower limit and show postnatal and gestational age dependence. *Neonatology* 2012;102:68-74.
28. Snoeck V, Huyghebaert N, Cox E, Vermeire A, Saunders J, Remon JP, Verschooten F, et al. Gastrointestinal transit time of nondisintegrating radio-opaque pellets in suckling and recently weaned piglets. *J Control Release* 2004;94:143-153.
29. Janas MM, Wang B, Harris AS, Aguiar M, Shaffer JM, Subrahmanyam YV, Behlke MA, et al. Alternative RISC assembly: binding and repression of microRNA-mRNA duplexes by human Ago proteins. *RNA* 2012;18:2041-2055.
30. Melnik BC, Kakulas F, Geddes DT, Hartmann PE, John SM, Carrera-Bastos P, Cordain L, et al. Milk miRNAs: simple nutrients or systemic functional regulators? *Nutr Metab (Lond)* 2016;13:42.
31. Thorell L, Sjoberg LB, Hernell O. Nucleotides in human milk: sources and metabolism by the newborn infant. *Pediatr Res* 1996;40:845-852.

32. Weil PP, Jaszczyszyn Y, Baroin-Tourancheau A, Postberg J, Amar L. Holistic and Affordable Analyses of MicroRNA Expression Profiles Using Tagged cDNA Libraries and a Multiplex Sequencing Strategy. *Methods Mol Biol* 2017;1654:179-196.
33. Livak KJ, Schmittgen TD. Analysis of relative gene expression data using real-time quantitative PCR and the 2(-Delta Delta C(T)) Method. *Methods* 2001;25:402-408.
34. Blankenberg D, Von Kuster G, Coraor N, Ananda G, Lazarus R, Mangan M, Nekrutenko A, et al. Galaxy: a web-based genome analysis tool for experimentalists. *Curr Protoc Mol Biol* 2010;Chapter 19:Unit 19 10 11-21.
35. Giardine B, Riemer C, Hardison RC, Burhans R, Elnitski L, Shah P, Zhang Y, et al. Galaxy: a platform for interactive large-scale genome analysis. *Genome Res* 2005;15:1451-1455.
36. Goecks J, Nekrutenko A, Taylor J, Galaxy T. Galaxy: a comprehensive approach for supporting accessible, reproducible, and transparent computational research in the life sciences. *Genome Biol* 2010;11:R86.
37. Vitsios DM, Enright AJ. Chimira: analysis of small RNA sequencing data and microRNA modifications. *Bioinformatics* 2015;31:3365-3367.
38. Aparicio-Puerta E, Lebron R, Rueda A, Gomez-Martin C, Giannoukakos S, Jaspez D, Medina JM, et al. sRNAbench and sRNAtoolbox 2019: intuitive fast small RNA profiling and differential expression. *Nucleic Acids Res* 2019;47:W530-W535.
39. Nelson PT, De Planell-Saguer M, Lamprinaki S, Kiriakidou M, Zhang P, O'Doherty U, Mourelatos Z. A novel monoclonal antibody against human Argonaute proteins reveals unexpected characteristics of miRNAs in human blood cells. *RNA* 2007;13:1787-1792.
40. Kratzer RF, Kreppel F. Production, Purification, and Titration of First-Generation Adenovirus Vectors. *Methods Mol Biol* 2017;1654:377-388.
41. Blankenberg D, Gordon A, Von Kuster G, Coraor N, Taylor J, Nekrutenko A, Galaxy T. Manipulation of FASTQ data with Galaxy. *Bioinformatics* 2010;26:1783-1785.

42. Kim D, Pertea G, Trapnell C, Pimentel H, Kelley R, Salzberg SL. TopHat2: accurate alignment of transcriptomes in the presence of insertions, deletions and gene fusions. *Genome Biol* 2013;14:R36.

## Figures and legends

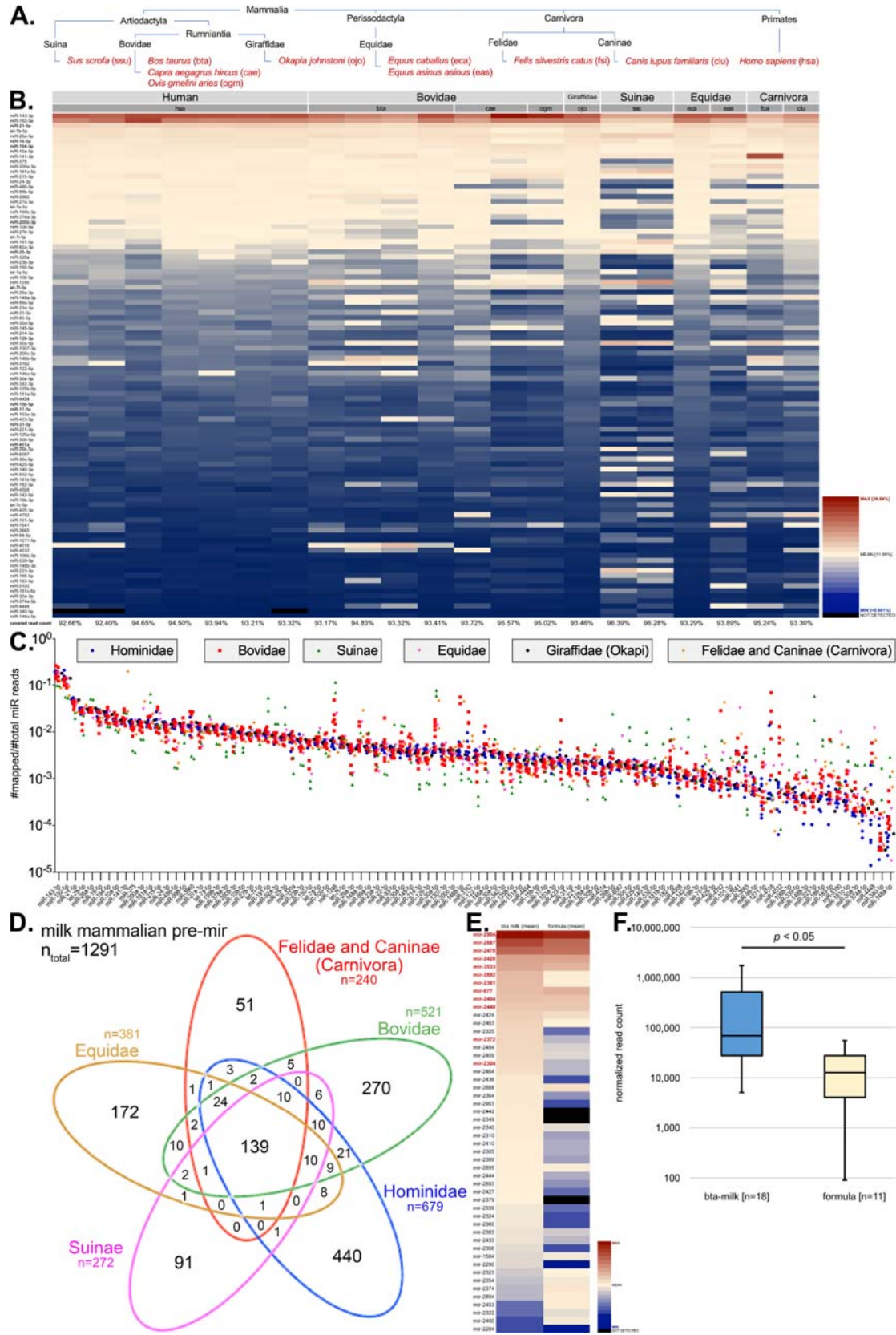


**Figure 1.** *Comparative profiling of mammalian milk miRNAs.* **A.** Phylogenetic tree of specimens under analysis (red font), which included mostly domesticated species with the exception of okapi (ojo) and human (hsa). Additionally, we determined miRNA profiles from yak cheese and water buffalo cheese (light red font), which are part of the available dataset, but are not part of the below analyses due to insufficient total read counts and quality. **B.** Heat map of miRNAs conserved in all taxa analysed. Only the top 100 miRNAs found in all species are shown robustly representing over 90% of the total read count in all specimens (see values below each column). A colour gradient was used for the visualisation of each miRNA's abundance (read counts per million; CPM) in each specimen. MicroRNAs were sorted in descending order with reference to the median CPM of human specimens. **C.** The chart illustrates the quantitative distribution of the same top 100 miRNAs shown in the above heat map. **D.** Venn diagram showing that the numbers of pre-miRNAs (pre-mir) shared by all or some taxa or, respectively, which were identified being taxon-specific. For this analysis pre-mir counts were used rather than miR-counts to counteract a potential differential taxon-specific 5p-/3p-dominant processing. **E.** Heat map of the top 50 *Bos taurus* (bta)-specific pre-mir in raw and industrially processed milk specimens (n=18) in comparison with powdered milk/formula product specimens (n=11). The median CPM (mapped reads count per million) was used as sorting criterion in descending order. Red font: miRNA was used for human mRNA target prediction via the sequence-based custom prediction option of miRDB (26). Cave! Bovidae in heat map include goat and sheep, whereas ranks were determined from cattle only. **F.** Quantitative analysis of total miRNA read counts in raw and industrially processed milk specimens (n=18) in comparison with powdered milk/formula product specimens (n=11).

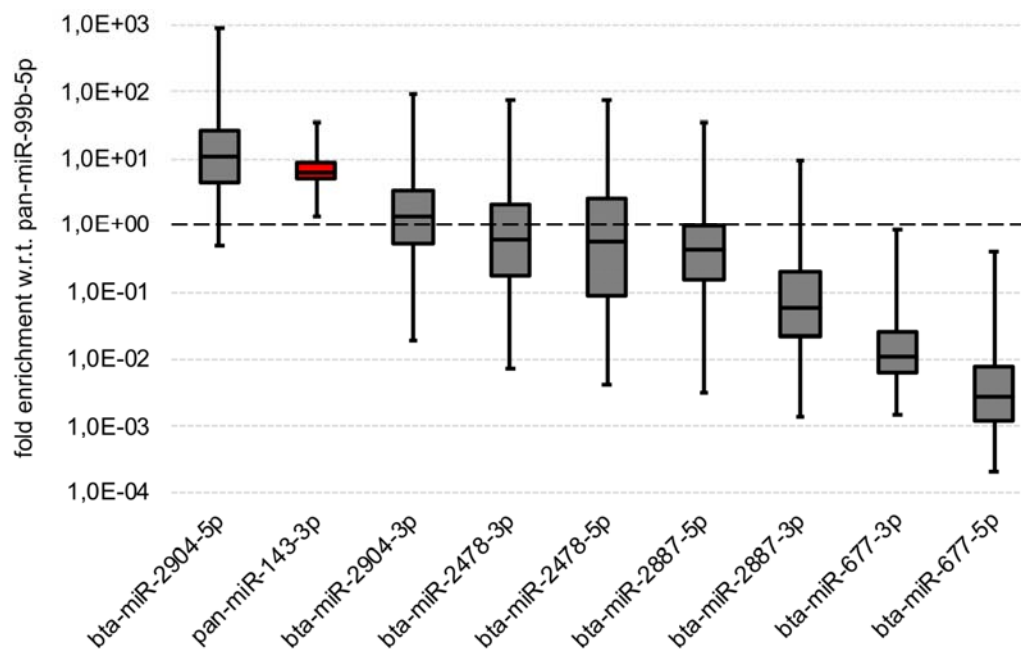


**Figure 2.** Xenobiotic bta-miRs survive the gastrointestinal passage in preterm neonates. **A.** Results of qPCR for selected bta-miRs. For comparison, pan-miR-143-3p shared by humans and cattle is shown (red box). The relative enrichment was normalized with respect to pan-miR-99b-5p.



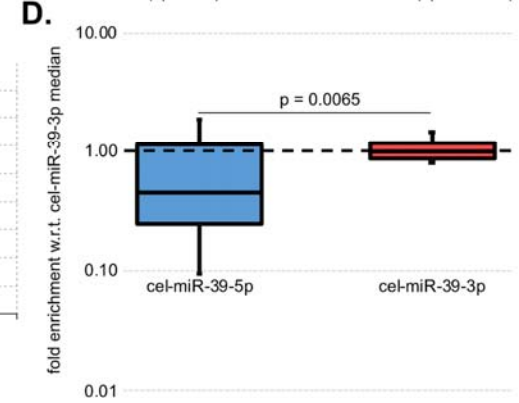
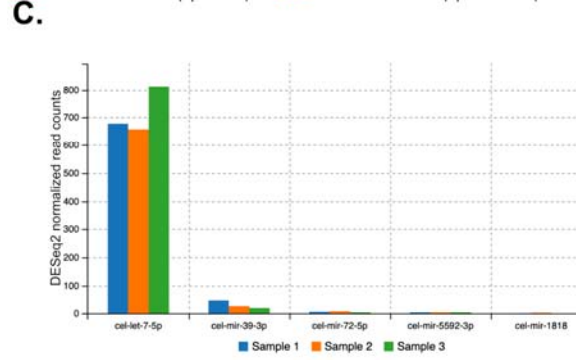
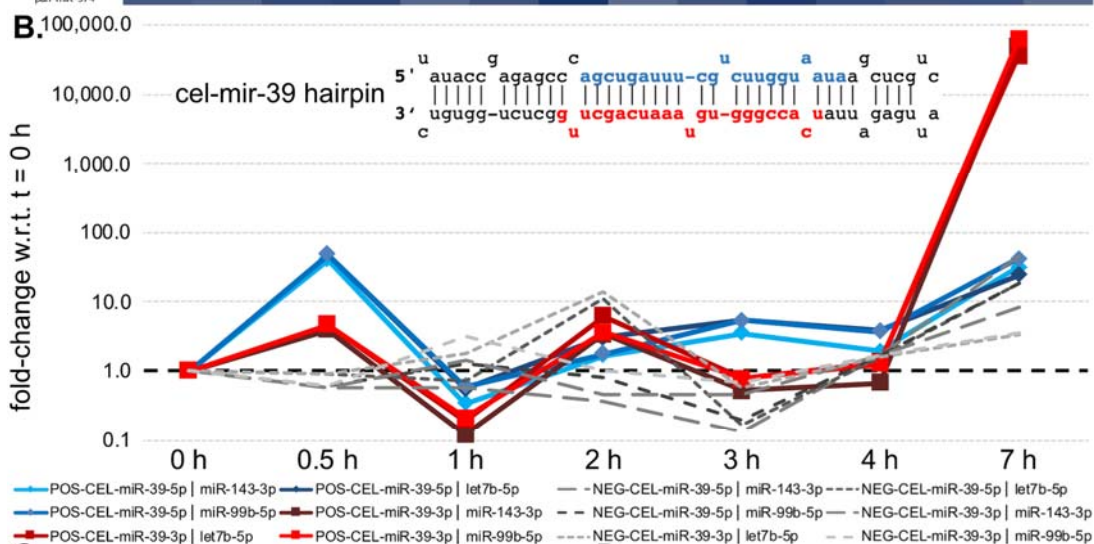
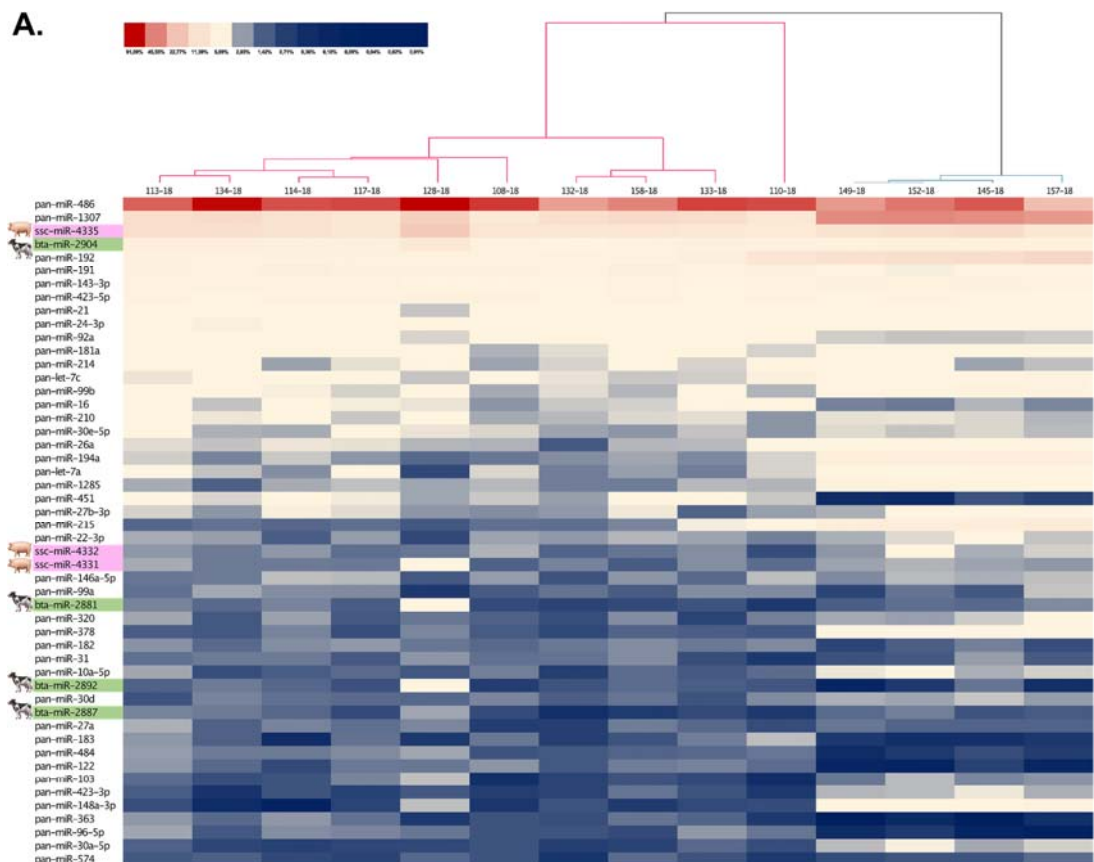




**Figure 3.** Reporter *cel-miR-39-3p* accumulates in the bloodstream and *cel-miR-39-5p/-3p* co-precipitate with Argonaute/Ago2 from homogenized intestinal biopsies. **A.** Heat map of miRNAs detected in enriched porcine preterm neonatal intestinal cells following 9 days of enteral bovine colostrum/formula supplementation. Only the top 50 miRNAs found in all species are shown. A colour gradient was used for the visualisation of each miRNA's abundance (read counts per million; CPM) in each specimen. MicroRNAs were sorted in descending order with reference to the median CPM of all specimens. **B.** *C. elegans* (*cel*)-mir-39 hairpin. Prospective guide and passenger strands are highlighted for *cel-miR-39-5p* (blue) and *cel-miR-39-3p* (red). **C.** Results of qPCR. Normalization of *cel-miR-39-5p* and *cel-miR-39-3p* was performed using endogenous pan-miR-143-3p, pan-miR-99b-5p or pan-let-7b-5p, respectively. Blue curves: *cel-miR-39-5p* (POS; *cel-miR-39* feeding); red curves: *cel-miR-39-3p* (POS; *cel-miR-39* feeding); grey curves: (NEG; no *cel-miR-39* supplementation). **D.** Using Chimira (37) for analysis of small RNA sequencing raw data from piglet blood serum miRNAs and selection '*C. elegans*' as species option, we identified *cel-miR-39-3p* (avg. 95 raw read counts). For comparison, matching *cel-let-7-5p* (avg. 2145 raw read counts, sequence identity to *ssc-let-7a-5p* [nt 1-22]) and *cel-miR-72-5p* (avg. 22 raw read counts, probably being identified as *ssc-miR-31-5p* [1nt mismatch]) are shown as well as ambiguous matches for *cel-miR-5592-3p* (avg. 17 raw read counts) and *cel-miR-1818* (avg. 5 raw read counts). Notably, the charts y-axis is DESeq2 normalized read counts. **E.** Results of qPCR after Argonaute pull-down using monoclonal mouse pan-argonaute/Ago2 antibodies (Sigma-Aldrich, MABE56, clone 2A8 (39)) and detection of reporter miRs by qPCR from miRNA libraries prepared from co-precipitated small RNAs.

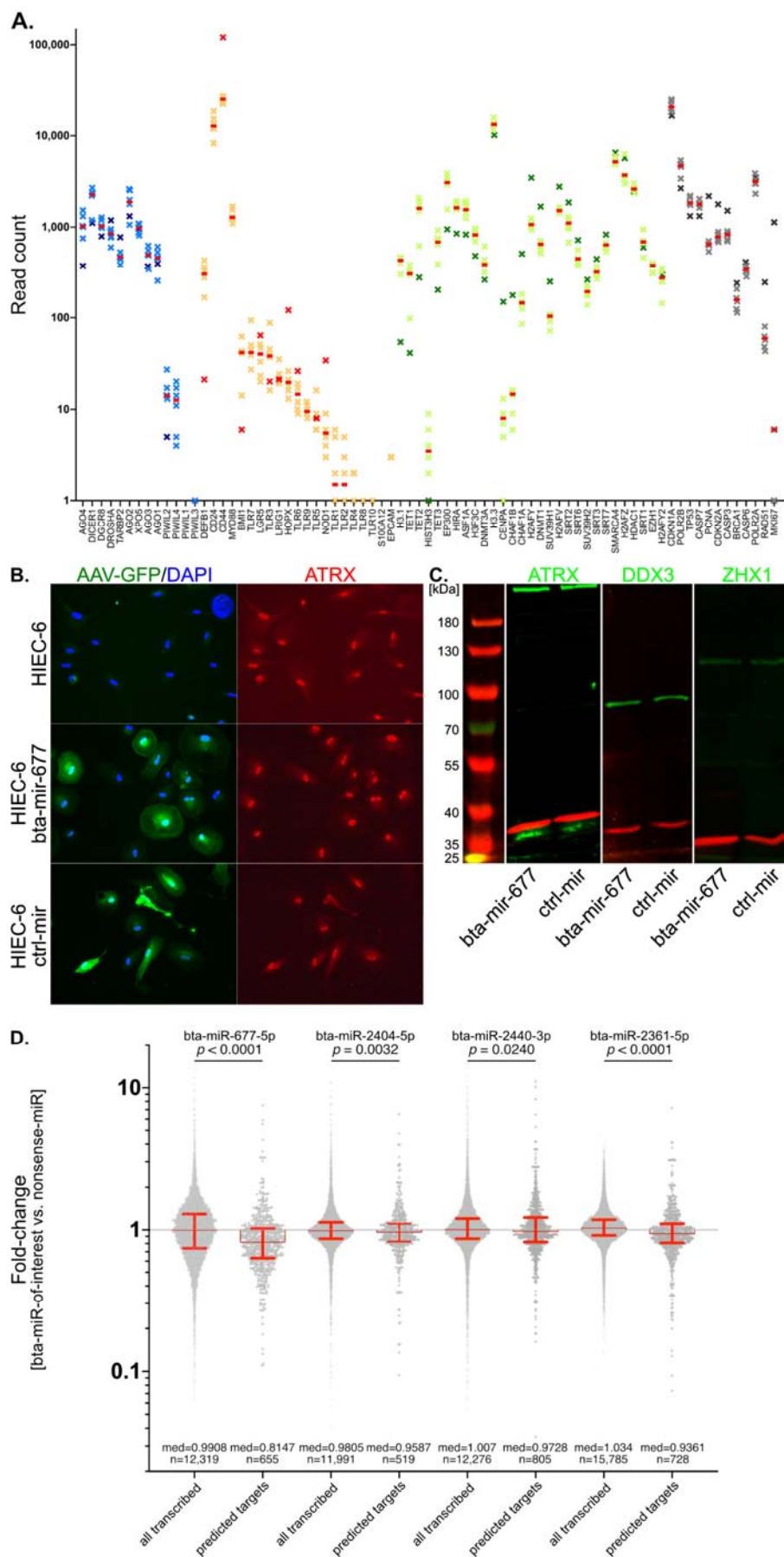


**Figure 4.** Tests for the suppression of predicted human mRNA targets of bta-miR-677 on the protein level for selected candidates and for 4 bta-miRs on the whole transcriptome level. **A.** Mapped raw read counts reflect HIEC-6 gene expression profiles. Selected groups of genes are shown: gene expression related to miRNA biogenesis and RNAi activity (blue asterisks), intestinal epithelial cell markers and innate immunity gene expression (orange asterisks); DNA methylation and chromatin structure related gene expression (green asterisks); cell cycle and proliferation related gene expression (grey asterisk). Untreated HIEC-6 are highlighted in each data column through darker coloured asterisks. Each red line marks the median read count for each data column. **B.** Immunofluorescence microscopy revealed no differences in the nuclear localisation of ATRX upon Ad5-mediated bta-miR-677 gene transfer into primary HIEC-6 cells. ATRX predominantly exhibited nuclear localisation and therein we observed focal accumulations in wt-HIEC-6 as well as in bta-mir-677-treated HIEC-6 and ctrl-mir-treated HIEC-6. We routinely focussed our view to areas wherein cells exhibited GFP-signals of different intensity. This should enable us to detect differences in ATRX distribution, which hypothetically could depend on the level of expressed bta-mir-677. Again, no differences were seen between treated cells and untreated controls. Notably, for PLCXD3 no reliable signals were observed in HIEC-6 cells at all. **C.** When normalized with the GAPDH, no differences in the abundances of ATRX or ZHX1 were observed upon Ad5-mediated bta-miR-677 gene transfer into primary HIEC-6 cells in Western analyses, when compared to wild-type (wt) HIEC-6 (not shown) or HIEC-6 expressing a control-mir. Using two replicative measurements for quantitative Western Blot analyses via LI-COR Empiria Studio Software, we measured a 24.45% (SD:  $\pm 1.68\%$ ) DDX3 signal reduction in bta-mir-677-treated vs. wt and, respectively, a 37.90% (SD:  $\pm 1.90\%$ ) DDX3 signal reduction in bta-mir-treated vs. ctrl-mir-treated HIEC-6. **D.** Effects of Ad5-mediated expression of 4 selected bta-miRs were studied in HIEC-6 (bta-miR-677-5p; bta-miR-2404-5p; bta-miR-2400-3p; bta-miR-2361-5p) in comparison to HIEC-6 expressing a Ad5-mediated nonsense-miR. Relative fold-changes were compared for the whole HIEC-6 transcriptome and the lists of expressed predicted targets. Predicted targets for each bta-miR comprised of hundreds of mRNAs (i.e. bta-miR-677-5p [n=655]; bta-miR-2404-5p [n=519]; bta-miR-2400-3p [n=805]; bta-miR-2361-5p [n=728]). Statistical power

calculations were done using the nonparametric Wilcoxon–Mann–Whitney method and GraphPad Prism 8.4.3 software.

## Supplemental Figures and Legends

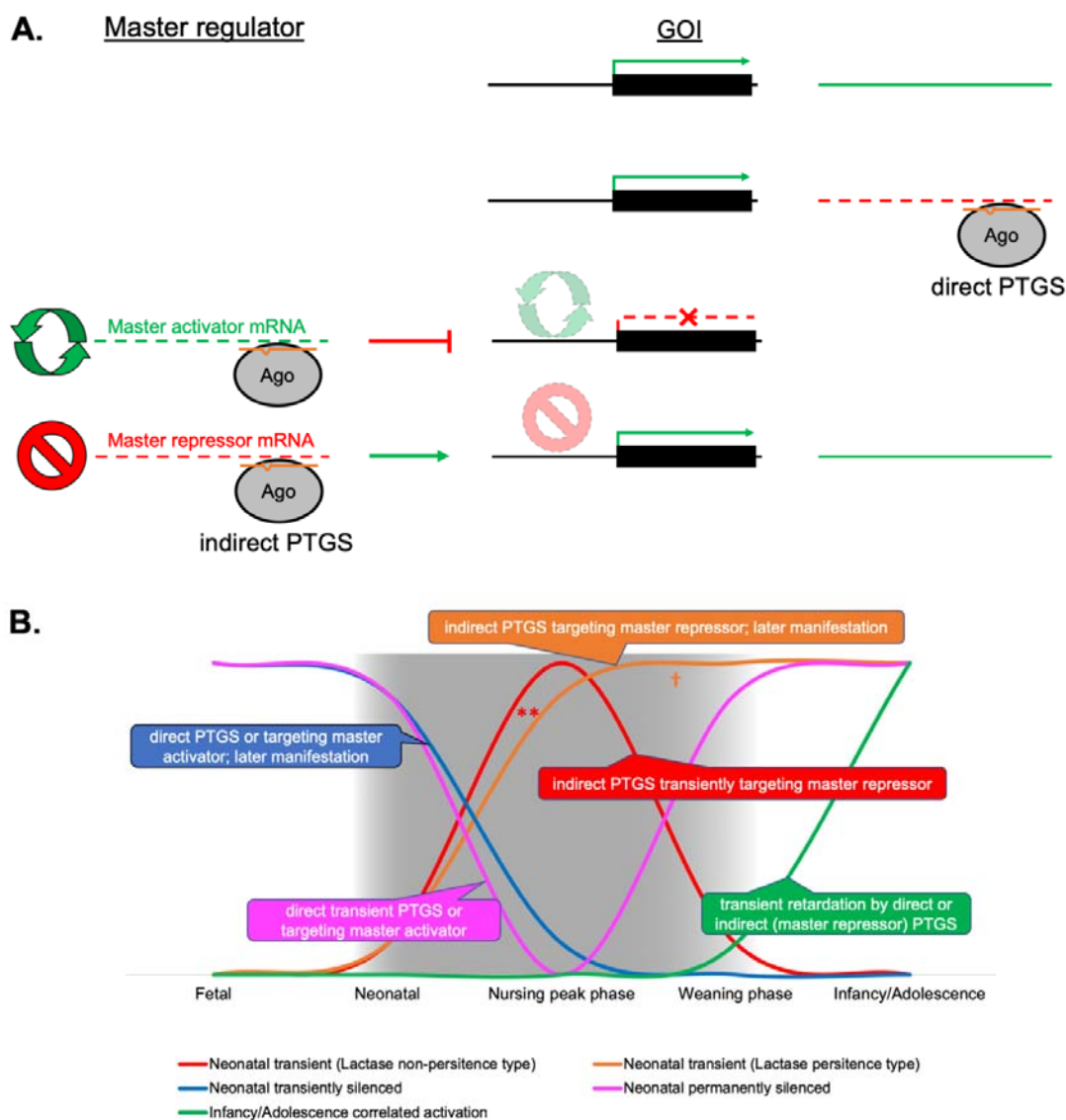


**Figure S1.** Illustration of theoretical regulatory contributions of breast milk microRNAs in the offspring. **A.** Posttranscription gene silencing (PTGS) depends on the targeting of mRNAs by microRNAs leading to their suppression through mRNA decay or translational blocking. With respect to any virtual gene-of-interest (GOI) a given microRNA can act directly on a GOI's mRNA or upstream in its regulatory hierarchy on a GOI's master activator's mRNA or, respectively, on a master

repressor mRNA. **B.** The regulatory contribution of breast milk microRNAs can theoretically explain any gene expression pattern observable during and around the nursing period.

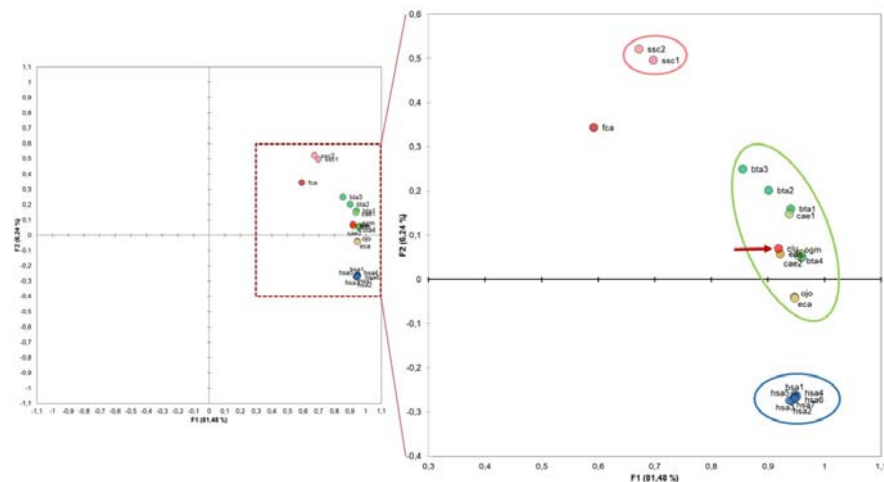


**Figure S2.** Results of principal component analyses of microRNAs shared by all taxa under investigation. Quadrants I and IV (section magnified on the right) harbour all specimens whereby all human specimens (blue: hsa1-7) are clustering. Slightly separated is a separated scattered cluster harbouring all herbivorous specimens (yellow to green: bta1-4, cae1-2, eas, eca, ogm, ojo) and one dog specimen (red arrow: clu). Above is a mini-cluster comprising both porcine specimens (pink: ssc1-2) and separated the cat specimen (red: fca).

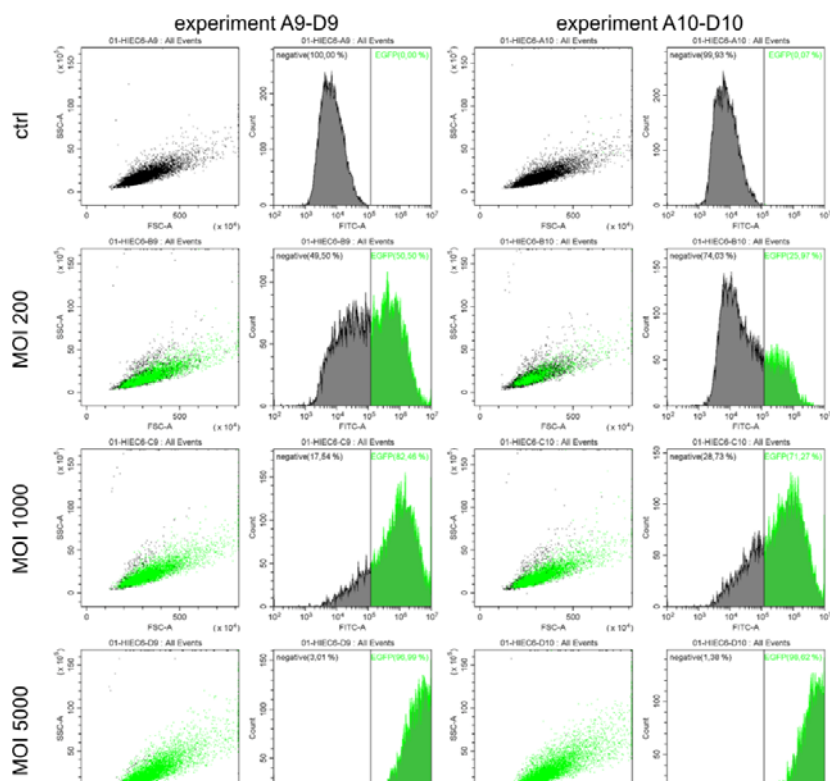


**Figure S3. Transduction efficiency.** The efficiency of Ad5-mediated gene transfer to HIEC-6 was measured by flow cytometry. Serial experiments using different MOIs (ctrl, 200, 1000, 5000) in two independent HIEC-6 culture batches (no. 9/10) are shown. Measurements of GFP-positive cells revealed that in HIEC-6 near quantitative transduction (>95% at a  $\text{MOI} \geq 5.000$ ) could be achieved 96h post-transduction

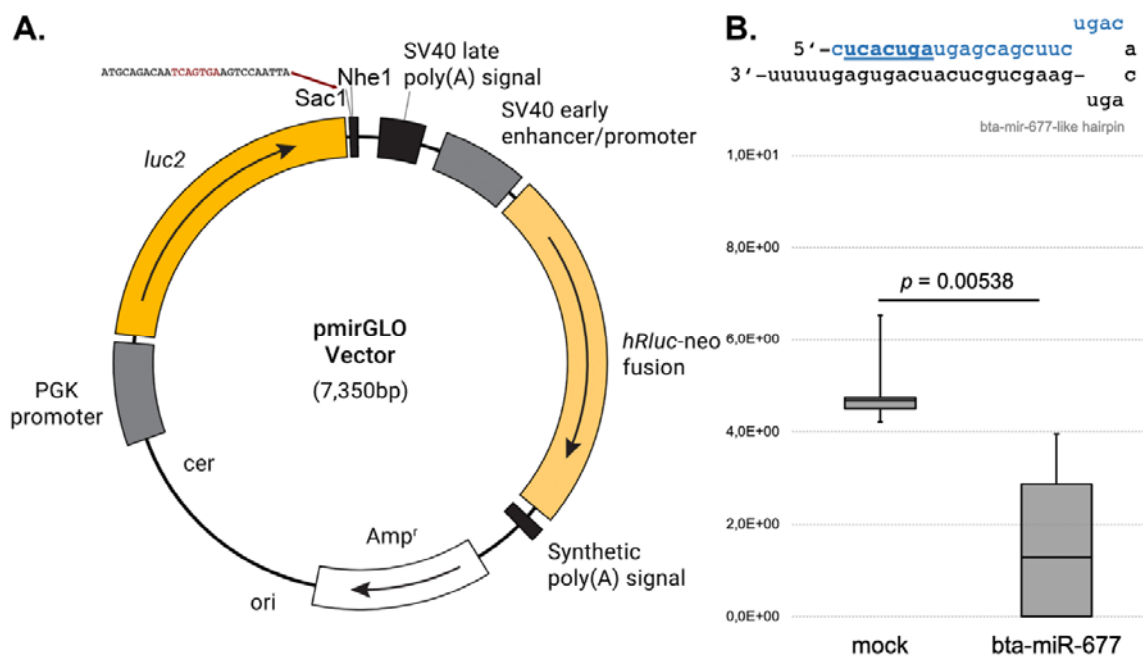


**Figure S4.** Activity tests for *bta-miR-677* using a predicted target sequence cloned into a luciferase 3'-UTR gene segment. **A.** Cloning of putative *bta-miR-677* target motif into the 3'-UTR region of the firefly luciferase gene using Sac1 and Nhe1 for restriction digest. **B.** Results of firefly luciferase silencing by *bta-miR-677*-like hairpin RNA co-transfected with pmirGLO (Promega) in HeLa cells. *Renilla* luciferase expression from the same vector was used for normalization in control experiments and upon *bta-miR-677*-like hairpin co-transfection. Altogether, 22 independent experiments (mock: n=11; *bta-miR-677* hairpin: n=11) were conducted.



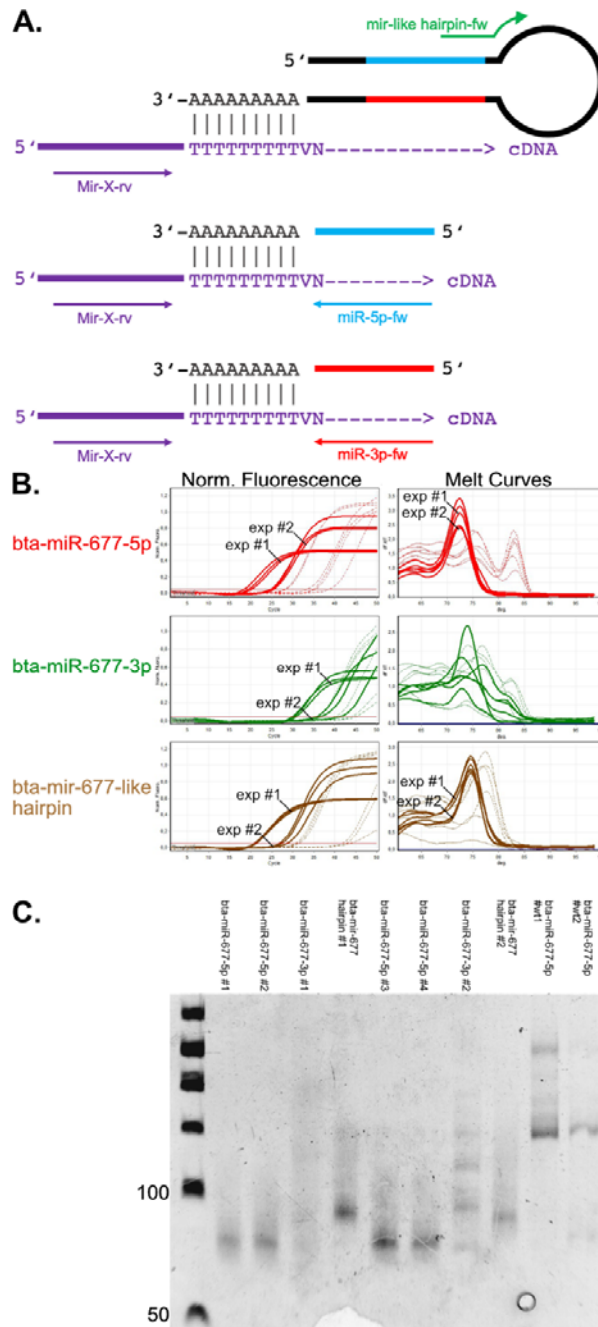


**Figure S5.** Tests for the presence of bta-mir-677-like hairpins and mature bta-miR-677-5p or bta-miR-677-3p, respectively. Tests were performed using the Mir-X kit (Takara Bio USA, Inc.) in combination with qPCR and PAGE. **A.** Briefly, poly[A] polymerase was used to tail the 3'-ends of microRNA precursors and mature microRNAs. Subsequently, 5'-adaptored oligo[T]VN was used to prime cDNA synthesis. For qPCR forward primers discriminating precursors and mature microRNAs were used in combination with Mir-X proprietary adaptor-specific reverse primers. **B.** The use of forward primers for mature bta-miR-677-5p (red curves) as well as the bta-mir-677-like hairpin



(brownish curves) resulted in reproducible  $C_T$  values associated with sharp melting curves in different experiments, whereas the use of primers for mature bta-miR-677-3p resulted in probably unspecific signals (concluded from the irregular melting curves). Control experiments using RNA from wildtype HIEC-6 did not produce reproducible qPCR signals and melting curves (dashed lines in all charts). **C.** The PCR amplicons were separated by PAGE (6% PAA) in order to confirm the predicted size shift between microRNA precursors and mature microRNAs, respectively. The band sizes of the mature bta-miR-677-5p (expected size between 60 and 70 bp) as well as the observed shift with respect to the bta-mir-677-like (hairpin) precursor were in agreement with the theoretical expectations, whereas no specific amplicon could be seen for bta-miR-677-3p and wildtype control experiments.